



Intrinsic functional network architecture of human semantic processing: Modules and hubs



Yangwen Xu, Qixiang Lin, Zaizhu Han, Yong He, Yanchao Bi*

National Key Laboratory of Cognitive Neuroscience and Learning & IDG/McGovern Institute for Brain Research, Beijing Normal University, Beijing 100875, China

ARTICLE INFO

Article history:

Received 19 August 2015

Accepted 3 March 2016

Available online 10 March 2016

Keywords:

Functional connectivity

Connectome

Default mode network

Language

Semantic control

Semantics

ABSTRACT

Semantic processing entails the activation of widely distributed brain areas across the temporal, parietal, and frontal lobes. To understand the functional structure of this semantic system, we examined its intrinsic functional connectivity pattern using a database of 146 participants. Focusing on areas consistently activated during semantic processing generated from a meta-analysis of 120 neuroimaging studies (Binder et al., 2009), we found that these regions were organized into three stable modules corresponding to the default mode network (Module DMN), the left perisylvian network (Module PSN), and the left frontoparietal network (Module FPN). These three dissociable modules were integrated by multiple connector hubs—the left angular gyrus (AG) and the left superior/middle frontal gyrus linking all three modules, the left anterior temporal lobe linking Modules DMN and PSN, the left posterior portion of dorsal intraparietal sulcus (IPS) linking Modules DMN and FPN, and the left posterior middle temporal gyrus (MTG) linking Modules PSN and FPN. Provincial hubs, which converge local information within each system, were also identified: the bilateral posterior cingulate cortices/precuneus, the bilateral border area of the posterior AG and the superior lateral occipital gyrus for Module DMN; the left supramarginal gyrus, the middle part of the left MTG and the left orbital inferior frontal gyrus (IFG) for Module FPN; and the left triangular IFG and the left IPS for Module PSN. A neuro-functional model for semantic processing was derived based on these findings, incorporating the interactions of memory, language, and control.

© 2016 Elsevier Inc. All rights reserved.

Introduction

Semantic processing is central to many cognitive functions, such as language, thought, object recognition, and use. It is a highly complex faculty, including a storage of semantic knowledge, tightly related to language (Berwick et al., 2013), memory, and sensorimotor systems (Barsalou, 1999; Barsalou et al., 2003), which can be retrieved or manipulated in a dynamic fashion by the control system (Badre et al., 2005; Noonan et al., 2013; Thompson-Schill et al., 1997; Wagner et al., 2001; Whitney et al., 2011, 2012). These systems are integrated to achieve the semantic function (Binder and Desai, 2011; Dove, 2009, 2010; Jefferies, 2013; Paivio, 1990; Vigliocco et al., 2009; Zwaan, 2014). A careful and comprehensive meta-analysis of 120 functional neuroimaging studies (Binder et al., 2009) identified brain areas consistently activated during semantic processing mainly including the inferior parietal lobe, the middle temporal gyrus, the fusiform and parahippocampal gyri, the dorsomedial prefrontal cortex, the inferior frontal gyrus, the ventromedial prefrontal cortex, and the posterior cingulate gyrus.

It is commonly assumed that these distributed regions that are reliably activated in semantic tasks are connected as a unified network to support semantic processing (Binder et al., 2009; Fang et al., 2015; Han et al., 2013; Saur et al., 2008; Turken and Dronkers, 2011). While multiple white matter pathways have been identified as the anatomical backbone of this semantic processing network with potential modular structures (Fang et al., 2015; Han et al., 2013; Saur et al., 2008; Turken and Dronkers, 2011), the exact pattern in which these regions are functionally connected remains unknown. Are these areas uniformly interconnected or further segregated into “modules” (i.e., more densely interconnected community) supporting different aspects of semantic processing? Are there regions more important than others in information integration, i.e., hubs (Buckner et al., 2009; Power et al., 2013; van den Heuvel and Sporns, 2013), in this semantic network? Several regions have been proposed to be the “hubs” of the semantic system, including the anterior temporal lobe as the “transmodal” site of the language system and multiple modality-specific systems (Lambon Ralph, 2014; Patterson et al., 2007; Rogers et al., 2004); the left angular gyrus, another heteromodal region (Bonner et al., 2013) which plays a critical role in conceptual combination (Price et al., 2015); and the left posterior middle temporal gyrus whose functional connectivity strengths with other regions are associated with semantic processing efficiencies (Wei et al., 2012). However, most of these proposals of

* Corresponding author.

E-mail address: ybi@bnu.edu.cn (Y. Bi).

“hubs” were based on theoretical analyses and indirectly inferred by testing their functions in isolation. Empirical studies of their special roles for semantic processing in terms of connectivity patterns are sparse.

The recent exciting development of human functional connectomic research (Biswal et al., 2010; Bullmore and Sporns, 2009; Smith et al., 2013; Sporns et al., 2005) provides us the opportunity to address these questions by unraveling the topological characters of the network using graph-theoretic approaches. Generally, a brain system will first be modeled as a graph composed of nodes and edges. The nodes represent functionally independent regions. The edges are usually defined as the interregional resting-state functional connectivity (RSFC), which is measured by the statistical coupling between the spontaneous fluctuations of the blood oxygen level-dependent signal of disparate regions (Biswal et al., 1995; Friston et al., 1993). Graph-theoretic methods offer measures to depict the features of the network established, including modules (He et al., 2009; Power et al., 2011; Yeo et al., 2011) and hubs (Buckner et al., 2009; Power et al., 2013; van den Heuvel and Sporns, 2013). While there are other network analysis techniques available, such as the independent component analysis, which has the advantages of revealing overlapping functional networks (Xu et al., 2013), the graph-theoretic approach directly addresses the network communication pattern and examines the nodal roles from the perspective of connectivity patterns.

This graph-theoretic approach was first applied to the semantic system by examining the wiring patterns among brain areas activated by associative semantic tasks (Vandenberghe et al., 2013), in which nodes were obtained by contrasting the main effect of verbal and non-verbal associative semantic tasks versus corresponding visual-perceptual tasks, and edges were defined as the effective connectivity during both semantic and perceptual task blocks. Modularity analyses on this network revealed six modules, including one matched with the language system and another consistent with the visual-perceptual system. The left pMTG with the left ventral occipitotemporal transition zone were visually identified as the regions bridging these two systems and the left posterior superior temporal sulcus was among the most densely connected regions within the language system. While this study provides intriguing clues about the dynamic effective connectivity patterns during one specific semantic task, important questions regarding the intrinsic semantic network architecture remain open: 1) The nodes were based on one type of semantic task contrast, which might be driven by certain aspects of semantic processing or even non-semantic components; 2) the edges were evaluated during both semantic or non-semantic task state, thus non-semantic information might be included; 3) different types of hubs were not explicitly identified using quantitative methods.

A comprehensive depiction of the semantic processing network that is not particularly biased to components specific to one particular task is greatly desired to help understand the intrinsic organizational principles of the semantic system. The goal of the present study is to construct such an intrinsic functional semantic processing network and use quantitative measurements to address two core questions: what are the systems in the semantic processing network, and what are the key regions integrating information within and across different systems? We derived nodes directly from the meta-analysis results in Binder et al. (2009), which was based on multiple types of semantic contrasts and specifically excluded confounding factors such as discordant control conditions or task difficulty differences. The edges were obtained by measuring the strengths of RSFC across these nodes using a database of 146 young healthy adults. After establishing the intrinsic functional semantic processing network, graph-theoretic approaches were performed to detect potential modules and hub regions important in within-module (provincial hubs) and across-module (connector hubs) information integration. Validations with an additional data session from a subgroup of the participants, a different preprocessing method, and an alternative way of defining nodes and edges were conducted to assess the stability of the main results.

Materials and methods

Participants

This study included 146 participants (70 males; 22.7 ± 2.1 years old) from the Connectivity-based Brain Imaging Research Database (C-BIRD) at Beijing Normal University. They were all right-handed (Li, 1983) with no history of neurological or psychiatric disorders. All participants provided written informed consents and were paid for their participation. This study was approved by the Institutional Review Board of the National Key Laboratory of Cognitive Neuroscience and Learning. The data of all 146 participants from the first resting-scan were used for main analyses. Notably, 57 of these participants underwent another resting-state scan after an interval of about 6 weeks (41.0 ± 4.5 days), which was used for the validation analyses (see “validation analysis” section). The validation dataset of these 57 participants is publicly available (Lin et al., 2015) (http://fcon_1000.projects.nitrc.org/indi/CoRR/html/bnu_1.html).

Image acquisition

Scans were performed on a 3 T Siemens Tim Trio scanner at the Beijing Normal University Imaging Center for Brain Research. High-resolution three-dimensional T1-weighted magnetization-prepared rapid gradient-echo images were acquired for anatomic reference [repetition time (TR) = 2530 ms, echo time (TE) = 3.39 ms, inversion time = 1100 ms, flip angle (FA) = 7° , 144 sagittal slices, voxel size = $1.33 \times 1 \times 1$ mm, field of view (FOV) = $192 \times 256 \times 256$ mm]. Functional images were obtained using an echo-planar sequence sensitive to blood oxygenation level-dependent contrast (TR = 2000 ms, TE = 30 ms; FA = 90° , 33 axial slices acquired interleaved with a 0.7 mm gap, voxel size = $3.125 \times 3.125 \times 4.2$ mm, FOV = $200 \times 200 \times 138.6$ mm, 200 volumes). Participants were instructed to stay awake and keep their eyes closed during the functional runs.

Data preprocessing

The imaging data preprocessing was implemented using Data Processing Assistant for Resting-State fMRI (DPARSF) (Yan and Zang, 2010) which is based on Statistical Parametric Mapping 8 (SPM 8: <http://www.fil.ion.ucl.ac.uk/spm>), including the following conventional steps: (1) discarding the first five time points allowing for signal equilibrium and adaptation of the participants to the scanning noise, (2) compensation of systematic slice-dependent time shifts, (3) correction for head movement with rigid body translation and rotation parameters, (4) normalization into Montreal Neurological Institute (MNI) space using unified segmentation on T1 weighted images and resliced into 3 mm cubic voxels, (5) spatial smoothing with 4 mm full-width half-maximum Gaussian kernel, (6) removing the signal trend with time linearly, (7) band-pass (0.01–0.1 Hz) filtering to decrease physiological noise, (8) regression of nuisance variables including six rigid head motion parameters, the global signal averaged across the whole brain, the white matter signal averaged from the deep cerebral white matter and the cerebrospinal fluid signal averaged from the ventricles to further reduce non-neuronal contributions. Images from two participants in the main dataset and another two participants in the validation dataset were excluded, for their maximum head motions were greater than 2 mm translation or 2° rotation.

Node definition

Nodes were derived based on the meta-analyses results of “all semantic contrasts” in Binder et al. (2009). We transformed this thresholded activation likelihood estimate (ALE) map (corresponding to Fig. 3 in Binder et al., 2009) from Talairach space into the MNI space using the “tal2icbm” transformation developed and validated by

Lancaster et al. (2007). Nodes were defined by building non-overlapping spheres around each peak voxel in the map. As peaks, especially those consistently identified across large collections of task-evoked neuroimaging studies, are assumed to act as activity epicenters for each functionally independent brain area, this method will better capture the underlying neurobiological properties than simply parcellating brain areas using anatomical borders (Power et al., 2011, 2013; Wig et al., 2011). Specifically, following Ekman et al. (2012), we started by building the first sphere (radius = 6 mm) around the peak in this map as the first node in the network. Then, we moved to the voxel with the next highest value to build the second sphere. A node was excluded if it overlapped with any previously generated nodes or extended beyond the gray matter mask, defined by voxels with a value higher than 0.4 in the SPM 8 gray matter probability template. After all the voxels within this map were exhausted, 60 nodes were generated.

Edge definition

Edges were defined as the interregional RSFC, computed by the Pearson correlation coefficient between the time courses of each pair of nodes. A node's time course was represented by the mean time course of all the voxels within that node. Thus, we generated a correlation matrix for each participant. These matrixes were Fisher z-transformed and averaged to form a mean RSFC matrix for the following analyses. The diagonal and negative links were set to zero following the convention (Power et al., 2011, 2013; Rubinov and Sporns, 2010), because it is questionable whether these negative RSFCs are biologically meaningful. Note that including the negative connections (by using their absolute values to reflect the connectivity strength) also did not alter our main result patterns. Also a range of thresholds were tested to exclude the weak links that may be spurious and obscure the topology of strong connections (Rubinov and Sporns, 2010). We set the connectivity density value (the proportion of survived links to all the possible links) at the lower limit when the graph began to fragment into components and increased it by 0.01 until 0.5 to test the results' stability across various thresholds. For the main dataset with global signal regression, the connectivity density ranged from 0.26 to 0.5. The corresponding functional connectivity strength varied from 0.28 to 0.12.

Module detection

To examine whether the semantic processing network is intrinsically organized into functionally specific systems, we performed a modularity analysis using the Graph-theoretical Network Analysis Toolkit (Wang et al., 2015) with the spectral optimization algorithm (Newman, 2006a, 2006b). This fast technique detects communities in graphs by maximizing the modularity Q , which is the measure of the goodness of a partition (Newman and Girvan, 2004). To test whether the modularity Q was significantly higher than those of random networks, a Z test was performed with the Q values generated from 10,000 random graphs constructed using the algorithm by Maslov and Sneppen (2002), which preserves the same number of nodes, edges, and the same degree distribution.

Hub detection

The degree centrality and participation coefficient (PC) were calculated to profile various aspects of nodal importance (Guimera and Nunes Amaral, 2005). The degree of node i was represented by $D_i = \sum_{j=1}^n A_{ij}$, where A was the adjacency matrix of a weighted graph containing n nodes. It could be an overall graph including all the modules (overall degree), two modules of interest, or one particular module that the node under consideration belonged to (within-module degree). This metric measured the centrality of a node interacting with other nodes

in a network. The PC of node i was calculated by $P_i = 1 - \sum_{s=1}^m \frac{D_{is}}{D_i}^2$, where m was the number of modules we focused on, D_{is} was the sum of edges connecting node i to all the nodes within module s , and D_i was the overall degree of node i within the modules we addressed. The PC value of a node tended to be one if the links to this node spread uniformly across the modules of interest and zero if the links were completely confined to one single module. These indexes were then normalized as the standard Z score.

Two types of hubs were identified: the connector hub and the provincial hub (Guimera and Nunes Amaral, 2005; Sporns et al., 2007). Connector hubs predominantly link different modules, whereas provincial hubs primarily connect nodes within their own modules. For connector hubs, we also distinguished the hubs connecting all three modules and those mainly linking specific pair of modules. To do so, we first identified the connector hubs for the overall network and then classified them into different types based on their connectivity strengths to each module. However, in this method, the regions that are important in connecting only two modules may not have chance to be detected. We thus adopted a second approach, in which connector hubs for each pair of modules were directly examined without considering the third module. Specifically, in the first "overall connector method," connector hubs for the overall network were defined as nodes with both high overall degree Z scores (>0.5) and PC Z scores (>0.5). Then the mean connectivity strength distribution of each connector hub across three modules (the average RSFC value from the hub node to all the nodes within each module) were calculated and the edge strength of the entire network (the sum of all the RSFC values in the network divided by the number of all the possible edges) were set as the threshold. Hubs with greater mean connectivity strength to all three modules were defined as the connector hubs of the entire network and those with higher mean connectivity strength to only two modules were treated as the connector hubs specially converging two according modules. In the second "module-pair connector method," the connector hubs linking each pair of modules were detected using the criteria that the degree Z score and PC Z score of the two modules under investigation were both greater than 0.5. The connector hubs for more than two pairs of modules were considered as those of the entire network. Provincial hubs were defined as nodes with a high within-module degree Z score (>0.5) but did not meet the criteria of connector hubs.

The location of hub regions were labeled referencing to the SPM anatomy toolbox (Eickhoff et al., 2005) when applicable, which contains the probabilistic cytoarchitectonic parcellation of the inferior parietal cortex (Caspers et al., 2006, 2008), the intraparietal sulcus (Choi et al., 2006; Scheperjans et al., 2008), and the Broca's region (Amunts et al., 1999).

Validation analyses

Four validation analyses were performed. 1) The replication data from another resting-state scan. Given that RSFC can be modulated by various factors, such as the emotional (Harrison et al., 2008) and cognitive state of the participants (Waites et al., 2005), an additional session of the data from a subgroup of the participants (see "Participants" section) were used to exclude the factors of participants' mental state. 2) A different preprocessing approach. While global signal regression significantly reduces the influence of head motion (Yan et al., 2013), there is a potential risk of introducing artifacts (Murphy et al., 2009) and removing biologically meaningful signals (Scholvinck et al., 2010). We thus repeated our analyses without global signal regression. 3) A different nodal resolution. The main analyses were conducted on the ROI level; we also generated nodes at the voxel level, in which we simply treated each voxel within the map as a node, generating 3138 nodes in total. Note that although the main scheme remained, the voxel-wised network was broken into more fragmented modules compared with the

modularity results at the ROI level under the same modularity resolution parameter ($\gamma = 1$). A lower modularity resolution parameter ($\gamma = 0.9$) was adopted at the voxel level for larger module detection in comparison with the results at the ROI level using the function within the Brain Connectivity Toolbox (Rubinov and Sporns, 2010). 4) Excluding short-range edges. Analyses were repeated by including only the long-range edges and setting short-range (Euclidean distance < 20 mm) ties to zero (Power et al., 2011, 2013). This approach was used because short-range edges might be spurious, resulting from data acquisition, preprocessing (smoothing and reslicing), and head motion (Power et al., 2012) rather than shared neuron activities.

Visualization

Network visualization was created using the Network Overview, Discovery and Exploration for Excel (Node XL, <http://nodexl.codeplex.com>) by the force-directed placement technique (Fruchterman and Reingold, 1991), in which the inter-nodal Euclidean distances reflected the graph-theoretic distance. Brain visualization was implemented with the BrainNet Viewer (Xia et al., 2013).

Results

Semantic processing network construction

The intrinsic functional semantic processing network was constructed by mapping the interregional RSFC among brain areas consistently activated across 120 functional neuroimaging studies focusing on semantic processing (Binder et al., 2009). By building 6 mm-radius spheres around peak voxels, 60 nodes (the center coordinates are presented in Table 1) were generated to cover all the key brain areas within the semantic meta-analysis map (Fig. 1A). These nodes were heavily connected into a unified network, as presented in Fig. 1B, under the connectivity density of 0.26, providing an intuitive view of the connectivity pattern.

Modules of the semantic processing network

To detect the potential modules within the semantic processing network, a community detection algorithm was applied on the mean RSFC matrix across various thresholds (i.e., connectivity density ranged from 0.26 to 0.5 with 0.01 increments). The modularity strengths (Q values), ranging between 0.22 and 0.27 across various thresholds, were all significantly greater than those of the random networks (Z scores ranged from 13.59 to 18.52; $p < 10^{-6}$, two tailed), indicating a strong modular structure (Supplementary Fig. 1). Following Power et al. (2011), we plotted the modular structure according to various connectivity density levels (Fig. 2A). Three modules were obtained, which were highly stable across all the thresholds examined. Fig. 2B–D illustrated the results under the connectivity density of 0.4, when all the nodes belonged to the most common modules across various thresholds. In the spring embedded layout (Fig. 2C), nodes were positioned in the plane according to their connectivity patterns. Well-connected nodes were grouped together, and un-tied nodes were pulled apart. These three modules were clearly distinguished from each other. In the functional connectivity matrix (Fig. 2D), three densely connecting clusters could be captured against with the background, indicating the stronger strength of within-module connections in comparison to the between-module ones.

The spatial locations of these three modules on brain surface are presented on Fig. 2B. The red-coded module mainly included the bilateral posterior cingulate cortices (PCC) with the adjacent precuneus, the bilateral medial prefrontal cortices (MPFC) that are close to the anterior cingulate cortices (ACC), the angular gyrus (AG), the superior lateral occipital cortex (SLOC), the left superior frontal gyrus (SFG), and a region centered on the middle part of left fusiform/parahippocampal

gyri. These areas covered the core regions of the default mode network (DMN) (Buckner et al., 2008; Greicius et al., 2003), which was considered as a memory-based simulation system (Buckner et al., 2008; Buckner and Carroll, 2007; Hassabis and Maguire, 2007; Schacter et al., 2007). The green-coded module primarily comprised the entire length of the left middle temporal gyrus (MTG), the orbital and triangular parts of the left inferior frontal gyrus (IFG), the middle frontal gyrus (MFG), the dorsal medial frontal gyrus (DMPFC), the left supramarginal gyrus (SMG), and the anterior part of left AG, which were almost within the left perisylvian network (PSN) (Friederici, 2011). These regions were treated as the “high-level” language processing system (Fedorenko et al., 2011; Fedorenko and Thompson-Schill, 2014), in contrast with other language-related regions serving sensorimotor and control processing. The blue-coded module contained the triangular part of the left IFG, the area around the left intraparietal sulcus (IPS), and a left inferior posterior temporal region, which mainly spread within the left frontoparietal network (FPN) (Dosenbach et al., 2008; Vincent et al., 2008). It has been shown that this left-lateralized control system is specifically involved in semantic control rather than more general control functions (Geranmayeh et al., 2012, 2014; Harel et al., 2014; Noonan et al., 2013; Whitney et al., 2011, 2012). We labeled these three modules as Module DMN, Module PSN, and Module FPN for convenience.

Hubs of the semantic processing network

Based on the findings of the three stable modules, we detected hubs within the semantic processing network with two metrics: the degree centrality and the PC (see “Material and methods”). Given that all these metrics were highly stable across various connectivity densities (Supplementary Fig. 2), the results under one particular threshold (connectivity density = 0.4, when all the nodes belonged to their most common modules across all the thresholds) are presented. Connector hubs responsible for cross-module communication and provincial hubs important in within-module integration were both identified.

Connector hubs

To distinguish the connector hubs converging all three modules and those only central to one specific pair of modules, two methods were used here (see “Material and methods”). For the “overall connector method,” we first detected the connector hubs of the overall network and then further judged whether these “overall” connector hubs preferred one specific pair of modules. As nodes merely important in connecting only two modules may be omitted in this method, we also directly examined the nodes critical to each pair of modules (“module-pair connector method”). These two methods yielded similar results.

Using the “overall connector method,” 11 nodes were identified as the “overall” connector hubs (overall degree Z score > 0.5 and overall PC Z score > 0.5). Based on the mean connectivity strength pattern across various modules, we classified these connector hubs into four types by setting 0.15 (the mean connectivity strength of the entire network) as the threshold (Fig. 3A). Adjacent nodes with the same tendency were treated as the same cluster. The connector hubs mainly linking Modules DMN and PSN were the bilateral ventral AG (specifically the cytoarchitectonic areas of PGp/PGa/PFm), the left anterior temporal lobe (ATL), and the left SFG; those primarily linking Modules DMN and FPN were the left dorsal portion of the posterior IPS (pIPS, specifically posterior to the cytoarchitectonic area of hIP3); and the one predominantly linking Modules PSN and FPN was the left posterior MTG (pMTG). Finally, the left AG (PGa/PGp) and the left MFG held strong connections with all three modules, indicating that they were the true overall connector hubs of all three modules.

The “module-pair connector method,” where the connector hubs of each pair of modules (i.e., with both high degree and PC Z Score > 0.5) of the two modules of concern) were detected directly, yielded similar

Table 1
Nodes of the semantic processing network. The MNI coordinate and its anatomical label on the automated anatomical labeling template (Tzourio-Mazoyer et al., 2002) of each node's center voxel are listed, sorted by their ALE values. The module and hub information illustrates the results under the connectivity density of 0.4 using the "overall connector method." (L = left, R = right, Mid = middle, Med = medial, Sup = superior, Inf = inferior, Orb = orbital, Tri = triangular).

Peak Order	Coordinates			Anatomical labels	Modules	Connector Hubs	Provincial Hubs
	X	Y	Z				
1	-45	-69	27	Angular_L	DMN	DMN&PSN	-
2	-48	-57	30	Angular_L	PSN	DMN&PSN	-
3	-48	-63	18	Temporal_Mid_L	PSN	-	-
4	-3	-57	18	Precuneus_L	DMN	-	✓
5	-60	-42	-3	Temporal_Mid_L	PSN	PSN&FPN	-
6	-45	30	-9	Frontal_Inf_Orb_L	PSN	-	✓
7	-60	-51	-9	Temporal_Mid_L	FPN	-	-
8	-33	-72	45	Parietal_Inf_L	DMN	DMN&FPN	-
9	-36	-78	33	Occipital_Mid_L	DMN	-	✓
10	-27	30	45	Frontal_Mid_L	DMN	-	-
11	-18	39	45	Frontal_Sup_L	DMN	DMN&PSN	-
12	-54	-63	9	Temporal_Mid_L	PSN	-	-
13	3	-57	27	Precuneus_R	DMN	-	✓
14	-42	-69	39	Angular_L	DMN	DMN&PSN&FPN	-
15	-30	-36	-15	Fusiform_L	DMN	-	-
16	-57	-48	6	Temporal_Mid_L	PSN	-	-
17	0	-57	45	Precuneus_L	DMN	-	-
18	48	-69	33	Angular_R	DMN	-	✓
19	57	-57	24	Temporal_Sup_R	DMN	DMN&PSN	-
20	-6	-51	33	Cingulum_Post_L	DMN	-	✓
21	-39	-48	48	Parietal_Inf_L	FPN	-	✓
22	-57	-51	30	SupraMarginal_L	PSN	-	✓
23	-39	24	-18	Frontal_Inf_Orb_L	PSN	-	-
24	-57	-12	-12	Temporal_Mid_L	PSN	DMN&PSN	-
25	-6	48	-6	Frontal_Med_Orb_L	DMN	-	-
26	-57	-54	15	Temporal_Mid_L	PSN	-	-
27	-48	18	6	Frontal_Inf_Tri_L	PSN	-	-
28	-12	-60	12	Calcarine_L	DMN	-	-
29	-45	27	21	Frontal_Inf_Tri_L	FPN	-	-
30	-54	-33	-3	Temporal_Mid_L	PSN	-	✓
Peak Order	Coordinates			Anatomical labels	Module	Connector Hubs	Provincial Hubs
X	Y	Z					
31	-54	-39	24	Temporal_Sup_L	PSN	-	-
32	-48	9	-21	Temporal_Pole_Sup_L	PSN	-	-
33	-3	-39	39	Cingulum_Mid_L	DMN	-	✓
34	63	-39	-3	Temporal_Mid_R	PSN	-	-
35	-36	24	42	Frontal_Mid_L	PSN	-	-
36	54	-48	12	Temporal_Mid_R	PSN	-	-
37	6	51	-6	Frontal_Med_Orb_R	DMN	-	-
38	-36	18	0	Insula_L	PSN	-	-
39	-39	42	-15	Frontal_Inf_Orb_L	FPN	-	-
40	-54	-3	-24	Temporal_Mid_L	PSN	DMN&PSN	-
41	-36	-60	45	Parietal_Inf_L	FPN	-	✓
42	-54	-24	-9	Temporal_Mid_L	PSN	-	✓
43	15	-57	6	Lingual_R	DMN	-	-
44	-54	-45	39	Parietal_Inf_L	FPN	-	-
45	-3	-69	24	Calcarine_L	DMN	-	✓
46	-18	30	51	Frontal_Sup_L	DMN	DMN&PSN	-
47	9	-48	36	Cingulum_Mid_R	DMN	-	✓
48	-3	48	21	Frontal_Sup_Medial_L	PSN	-	-
49	-24	21	51	Frontal_Mid_L	DMN	-	-
50	54	-63	15	Temporal_Mid_R	DMN	-	-
51	45	-63	42	Angular_R	DMN	-	-
52	-48	-54	42	Parietal_Inf_L	FPN	-	-
53	-24	-78	42	Occipital_Sup_L	DMN	-	-
54	-42	-78	21	Occipital_Mid_L	DMN	-	-
55	-51	18	24	Frontal_Inf_Tri_L	FPN	-	✓
56	-42	15	45	Frontal_Mid_L	PSN	DMN&PSN&FPN	-
57	-48	3	-33	Temporal_Inf_L	PSN	-	-
58	-36	-54	57	Parietal_Inf_L	FPN	-	-
59	57	-48	30	SupraMarginal_R	PSN	-	-
60	48	-72	21	Temporal_Mid_R	DMN	-	-

results (Supplementary Fig. 3): the connector hubs specific for Modules DMN and PSN were the left ATL and the left PCC; those for Modules DMN and FPN were the left pIPS; and the one for Modules PSN and

FPN was the left pMTG. Although there were no overlapping regions for connector hubs of different pairs of modules, the territory of the left AG and the left superior/middle frontal gyri clustered the connector

hubs of more than one pair of modules, which was in agreement with the results from the “overall connector method” that these two areas were the connector hubs linking all three modules.

Provincial hubs

The provincial hubs of each module were identified as nodes whose within-module degree Z score is greater than 0.5 but without meeting the requirement of connector hubs. These results are shown in [Fig. 3B](#). Adjacent nodes with the same tendency were treated as the same area. The provincial hubs of each module were located at the peripheral part of the junction of the temporal–parietal–occipital cortices (around AG), along with a set of other regions: the bilateral PCC/precuneus, the border area of the posterior AG (pAG, PGa/PGp), and the SLOC for

corresponded well with the functional systems in our current study. The Module DMN corresponds to the “module of medial temporal lobe (MTL),” the Module PSN overlaps with the “orbital frontal–temporal/occipital module,” and the Module FPN is consistent with the “opercular/triangular/middle frontal–subcortical module.” This function–structure correspondence further confirms the robustness of this modular segregation in the semantic system. Furthermore, the hub regions we detected using the resting-state data, such as the left AG, the left pMTG, the left IPS, and the left IFG, also appeared as hub regions during an associative semantic task (Vandenberghe et al., 2013), suggesting the general accordance between resting and task states. Note that one region that was discovered to be a hub in Vandenberghe et al. (2013), an area of left ventral occipitotemporal transition zone, was not included in the semantic meta-analysis results by Binder et al. (2009) and thus was not considered in our study. The hub regions we identified, especially the ATL, the left pMTG, and the left AG, correspond nicely with previous literature in various other context as critical regions for semantic processing, which motivated us to match the connectivity characteristics of these nodes with their special functions. In the following discussion, we reviewed the different functions of these three systems in semantic processing and related their functions to the two types of hub regions. We found that the provincial hubs tended to exhibit the same function of the systems they belonged to and the connector hubs showed the emerged function of the pairs of systems they connected. An integrative

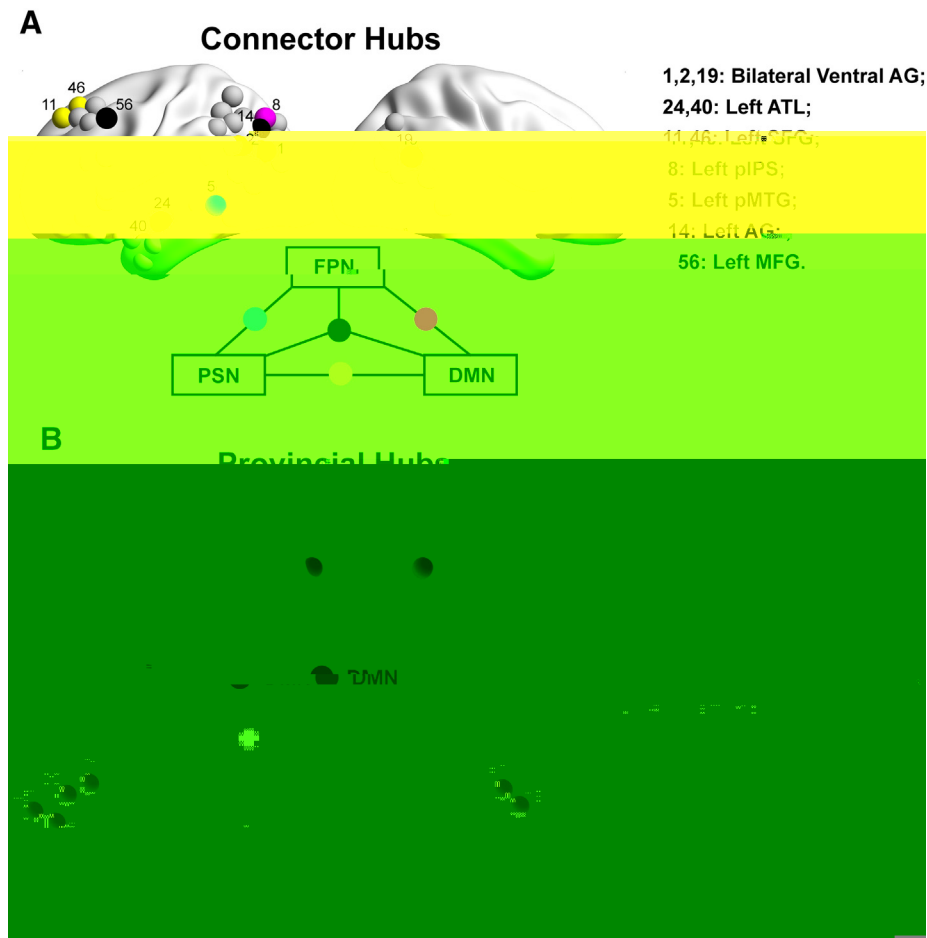


Fig. 3. Hub regions of the semantic processing network. These results were calculated under the connectivity density of 0.4, using the “overall connector method.” Hubs were painted with colors while other nodes were tinted light gray in the background. The labels of these hubs represent the peak order in Table 1. A) The connector hubs of the semantic processing network. As shown in the schematic figure, the connector hubs primarily connecting Modules DMN and PSN are colored yellow; those of Modules DMN and FPN are colored magenta; the one between Modules PSN and FPN is colored in cyan, the connector hubs of all three modules are in black. B) The provincial hubs of the semantic processing network. The provincial hubs of Module DMN are colored red, those of Module PSN in green, those of Module FPN in blue. (Prec = precuneus).

theory of mind (Carrington and Bailey, 2009; Spreng et al., 2009), and navigation (Spreng et al., 2009). A series of reviews proposed that the DMN can be best considered as a memory-based simulation system, serving to piece together materials from one's own past memories adapted for constructing new scenes, which can be self-projected into for evaluation, prospection and mentalization (Buckner et al., 2008; Buckner and Carroll, 2007; Hassabis and Maguire, 2007; Schacter et al., 2007). This system may be relevant for semantic processing in two ways. During system memory consolidation, this module's constituents, such as the ACC/MPFC, retrosplenial cortex and temporal lobes (Bontempi et al., 1999; Maviel et al., 2004; Tse et al., 2011), gradually capture the statistical structure of the multimodal experience, which is first converged and traced by the MTL system (McClelland et al., 1995; Squire and Alvarez, 1995). In this process, information is transformed from an episodic format to a more context-independent and semantic one (Nadel and Moscovitch, 1997; Winocur et al., 2007). In the reverse process, when a concept needs to be extracted, these brain areas will act as a simulator to re-enact the MTL system or further modality-specific brain areas (Barsalou, 1999; Barsalou et al., 2003), consciously (but not necessarily) providing sensorimotor or emotional experience of that concept in an egocentric manner. This mechanism is more plausible to represent concepts that are more imaginable and acquired from personal experience. Indeed, stronger activation has been observed for concrete object relative to abstract concepts (Binder et al., 2005; Sabsevitz et al., 2005; Wang et al., 2010), famous entities relative to common

items (Gorno-Tempini et al., 1998), and personal semantics relative to general semantics (Andrews-Hanna et al., 2010; Renoult et al., 2012). As the DMN has also been observed in nonhuman animals (Mantini et al., 2011) and the memory-based simulation function seems to exist in nonhuman animals even like rodents (Buckner and Carroll, 2007), this system may support a highly primitive form of “knowledge.” Of course, our analyses here are solely based on the RSFC patterns and the function of the DMN needs to be further investigated.

The provincial hubs of Module DMN were found at the bilateral PCC/precuneus and the bilateral pAG/SLOC. Bilateral PCC/precuneus is consistently found as the provincial hub of DMN (Power et al., 2013). The metabolic rate of this area is 40% greater than average (Raichle et al., 2001). Neuroimaging studies indicate its involvement in a substantial range of tasks including visuospatial imagery, episodic memory retrieval, and self-processing (Cavanna and Trimble, 2006; Vann et al., 2009). Focal damage to this region causes topographic disorientation and memory impairment (Leech and Sharp, 2014). Interestingly, Leech et al. (2012) have found that the ventral PCC showed strong functional connectivity with the rest of DMN whereas the dorsal part of this area showed high functional connectivity with the FPN, suggesting the PCC as a connector hub between these two networks. In our results, however, both parts were evaluated as the provincial hubs of the DMN (see also Power et al., 2013). The approach Leech et al. (2012) employed was specifically designed to investigate the unique functional connectivity patterns of different independent sub-regions within PCC

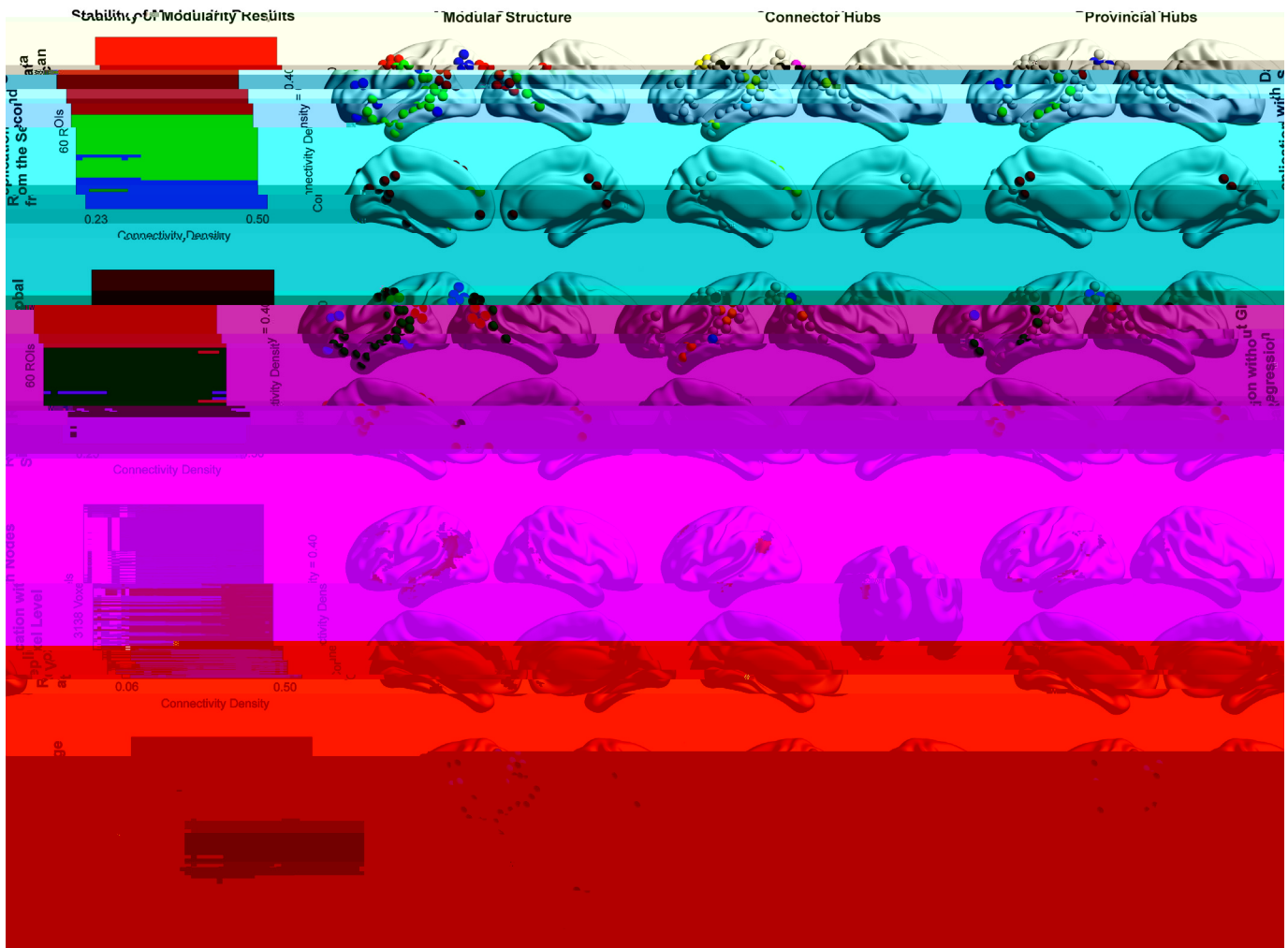


Fig. 4. Validation of the modularity and hub results. Column 1) shows the coherence of the modularity results under various thresholds across multiple validation analyses. The connectivity density starts when all the nodes in the network are fully connected to the value of 0.5. Modules containing similar brain areas across various thresholds are painted with the same color. The small fragmented modules, which do not spread across multiple thresholds, are all painted white, as shown in the voxel-level network when the thresholds are sparse. Three stable modules emerge from all the validation analyses. Column 2) presents the brain surface graph illustrating the locations of the three modules under a typical threshold in which each node belongs to the most common module across all thresholds. The spatial distributions of the three modules are similar across validations. Columns 3) & 4) show the validation of the connector and provincial hubs using the “overall connector method,” respectively, under the same connectivity density. The connector hubs primarily connecting Modules DMN and PSN are colored yellow; those of Modules DMN and FPN are colored magenta; the one between Modules PSN and FPN is colored cyan; the connector hubs of all three modules are in black. The provincial hubs of Module DMN are colored red; those of Module PSN are colored green; of Module FPN are colored blue. The other nodes are tinted light gray in the background.

and the common signal was regressed out. The potential further distinctions within PCC thus warrant further examination. For the other DMN provincial hub, the border area of the posterior AG and the lateral occipital gyrus, which extends to the transverse occipital sulcus, is strongly involved in scene processing (Dilks et al., 2013; Ganaden et al., 2013). The functions of these two areas coincide with those of DMN.

Module PSN as the language-based semantic system

Unlike DMN, Module PSN is almost left-lateralized, covering the entire length of MTG, the SMG, the anterior part of AG, DMPFC, and the orbital and triangular parts of the left IFG. These regions mainly correspond to the “core” or “high-level” language processing system proposed recently (Fedorenko et al., 2011; Fedorenko and Thompson-Schill, 2014), which is more strongly activated by language tasks contrasted with math, working memory, cognitive control, or music tasks (Fedorenko et al., 2011) and is distinguished from the peripheral language-related sensorimotor systems such as the visual word form area (Dehaene and Cohen, 2011; McCandliss et al., 2003), and the speech perception and

production regions (Hickok and Poeppel, 2007). This system serves to represent lexical (– semantic) items and syntactic rules and may act as an interface between the external language-related sensorimotor system and the internal mental world (Berwick et al., 2013), which is simulated by DMN. As processing the meanings of abstract and idiomatic concepts relies heavily on the linguistic context and needs more control demand (Hoffman, 2015), this system, as well as the control system (see below), is involved in processing these types of concepts in contrast with concrete (Binder et al., 2005; Sabsevitz et al., 2005; Wang et al., 2010) and literal (Boulenger et al., 2009; Lauro et al., 2008) concepts.

The provincial hubs of this module were the orbital part of the left IFG, the left mMTG and the left SMG. The mid part of the left MTG is the region with the most widely distributed functional connectivity and the richest structural connectivity patterns within the language network (Turken and Dronkers, 2011). Lesions in this site are associated with severe language comprehension deficits, especially on the single-word level (Dronkers et al., 2004). The orbital part of the IFG and the left SMG, which are also well connected, are located at the intersection

of the dorsal and ventral language pathways (Friederici and Gierhan, 2013; Saur et al., 2008). They are considered to be the regions for syntactic and semantic integration (Friederici, 2011).

Module FPN as the semantic control system

Module FPN encompassed the triangular part of the left IFG, the area around left IPS and the left inferior posterior temporal region. The FPN is considered as a flexible hub (Cole et al., 2013), providing the rapid adaptive control (Dosenbach et al., 2008) over the other functional systems. Specially, the left FPN has been considered to be involved in conceptual- and language-related control (Geranmayeh et al., 2012, 2014; Harel et al., 2014; Smith et al., 2009) and modulated by the difficulty of semantic tasks (Badre et al., 2005; Noonan et al., 2013; Thompson-Schill et al., 1997; Wagner et al., 2001; Whitney et al., 2011, 2012), whereas the right FPN is more engaged in the perceptual domain (Buxbaum et al., 2004; Harel et al., 2014). Note that this control function may differ according to which module it interacts with. To interact with Module DMN, the semantic control system helps to shift our attention of memory images to different modalities and different aspects of a given concept according to the task cues, in which a more posterior dorsal part of IPS is engaged (see the discussion of *pIP5*); To interact with the language-based semantic system, the control function serves to access the correct meaning of language depending on different task and language contexts, in which an additional posterior temporal region is involved (see the discussion of *pMTG*). Intriguingly, both in our study and many others (Geranmayeh et al., 2012, 2014; Power et al., 2013; Smith et al., 2009; Yeo et al., 2011), a left inferior posterior temporal region has been consistently detected to stick to other regions of the left FPN. Given its proximity to *pMTG*, the connector hub between Modules FPN and PSN (see below), they may share similar functions.

Again, the provincial hubs – the triangular part of the left IFG and the left IPS – have been shown to reflect the general function of this module. The triangular part of the left IFG we detected was located at the border area of BA44 and BA 45. Unlike the orbital part of the left IFG (BA 47), which was found to be the provincial hub of Module PSN and more engaged in controlled semantic retrieval (Wagner et al., 2001), this triangular part of IFG is sensitive to a broader range of semantic manipulation, including the semantic association strength and the semantic feature selection (Badre et al., 2005). Another region, the left IPS, is the area activated during top-down attention, in contrast to the ventral part that is involved in bottom-up attention (Corbetta and Shulman, 2002; Humphreys and Lambon Ralph, 2014). This region is also modulated by the difficulty of the semantic tasks (Humphreys et al., 2015; Noonan et al., 2013).

Integration across modules

ATL: The integration of the memory-based simulation system and the language-based semantic system

Wernicke (1900, as cited in Eggert, 1977) proposed that semantic knowledge arises from the interaction of our memory images and words, which still serves as a common framework for the semantic system (Binder and Desai, 2011; Dove, 2009, 2010; Paivio, 1990; Vigliocco et al., 2009; Zwaan, 2014). Our analyses showed that the left ATL, the left AG, and the left SFG are the key regions bridging the memory-based simulation system and the language-based semantic system. As the latter two regions coincided with connector hubs also for the semantic control system, their functions would be discussed below as the three module connectors. The ATL is probably the most famous candidate “hub” of semantic memory. This region is assumed to be the “transmodal” site of semantic features from multiple sensorimotor systems and the language system (Lambon Ralph, 2014; Patterson et al., 2007; Rogers et al., 2004). Its atrophy leads to both verbal and non-verbal semantic deficits in patients with semantic dementia (Bozeat et al., 2000; Garrard and Carroll, 2006; Hodges et al., 1992; Warrington, 1975). The function of this area corresponds to the fact that the left ATL

is one of the core regions of DMN (Buckner et al., 2008) and also consistently involved in language processing (Friederici, 2011), which is also what our current result highlights.

pMTG: The integration of the semantic control system and the language-based semantic system

The connector hub of the semantic control system and the language-based semantic system was located at the left *pMTG*, whose resting-state fluctuation amplitude has been shown to be associated with semantic processing efficiency in healthy populations (Wei et al., 2012).

level” linguistic
cause words
Hart and G
FPN (Geran
2013; Smith
demand of
Whitney et
interface b
based sema

pIP5: The in
simulation
control system
ages guided b



Fig. 5. The schematic framework of semantic processing. This model is based on our results (illustrated in the dashed line box; synthesizing results from the main analyses and the validation analyses) and a broad range of neuropsychological and functional neuroimaging findings. Functional systems with their provincial hubs are shown in rectangles, and connector hubs bridging these systems are illustrated in circles. (Tri = triangular; Orb = orbital; Prec = precuneus).

processing are quite sparse. The left SFG, which was identified as a connector hub of Modules DMN and PSN, is associated with self-introspection of outside stimuli (Goldberg et al., 2006; Gusnard et al., 2001). We speculate that this region may represent our self-reflective semantic knowledge. Considering the border area of the left SFG and MFG together, these regions and the supplementary motor area have common arterial supplies and are usually damaged together in ischemic stroke (Binder et al., 2009). Lesions in these areas cause transcortical motor aphasia (Freedman et al., 1984), a syndrome characterized by sparse self-initiated speech output but preserved semantic and grammatical abilities and unaffected repetition (Alexander, 2003). Binder and Desai (2011) proposed that this area plays a role in translating internal states into a coordinated plan for semantic knowledge retrieval. This process may be not only involved in self-guided production but also helps to predict the input elements during comprehension of both verbal and nonverbal stimuli (Pickering and Garrod, 2007).

The overall framework of semantic processing

A framework of semantic processing (Fig. 5) was derived synthesizing all the results. The semantic function is supported by three dissociable systems, which are integrated in the left AG and the border area of left SFG and MFG. Module DMN may act as a memory-based simulation system, in which the multimodal images converge and generalize. This system can re-enact the MTL system and further the modality-specific systems to instantiate the concepts acquired from our personal experience and guide our way of perception or action. Module PSN is involved in “high-level” language processing, which represents lexical items and syntactic rules. This system is interfaced with multiple peripheral language-related sensorimotor systems. These two systems interact in the left ATL where the semantic knowledge may emerge. Module FPN is engaged in the function of semantic control. This system provides adaptive control to the language-based semantic system through the left pMTG in order to retrieve the correct information during language processing, and to the memory-based simulation system via the left

pIPS, helping to shift our attention of memory images to different modalities and aspects. It is important to note, however, that this framework is indirectly inferred by the brain functions and their intrinsic connectivity patterns, and further empirical studies are needed to directly test each module and hub from this system-level perspective, as well as their dynamic topological patterns that associate with different types of semantic demands. The potential contribution of the subcortical nuclei, which have been implicated for semantic processing (Fang et al., 2015; Vandenberghe et al., 2013) and yet not included in the current analyses, also need to be considered in future studies.

Supplementary data to this article can be found online at <http://dx.doi.org/10.1016/j.neuroimage.2016.03.004>.

Funding

This work was supported by the National Basic Research Program of China (2013CB837300 to Y.B. and 2014CB846100 to Y.B. & Y.H.), National Natural Science Foundation of China (31221003 to Y.B. and 31271115 to Z.H.), National Science Fund for Distinguished Young Scholars (81225012 to Y.H.), Fok Ying Tong Education Foundation (141020 to Y.B.) and New Century Excellent Talents (12-0055 to Y.B. and 12-0065 to Z.H.).

Acknowledgments

We thank Dr. Jeffrey R. Binder for generously sharing the meta-analysis results reported in Binder et al. (2009). We also thank Alfonso Caramazza, Binke Yuan, Xiaosha Wang, Xiaoying Wang, and Yuxing Fang for helpful discussions and Chaogan Yan, Xindi Wang, and Xuhong Liao for technical assistance in data analysis.

References

- Addis, D.R., Wong, A.T., Schacter, D.L., 2007. Remembering the past and imagining the future: common and distinct neural substrates during event construction and elaboration. *Neuropsychologia* 45, 1363–1377.

- Alexander, M.P., 2003. 8 Transcortical motor aphasia: a disorder of language production. *Neurological Foundations of Cognitive Neuroscience*, p. 165.
- Alexander-Bloch, A., Lambiotte, R., Roberts, B., Giedd, J., Gogtay, N., Bullmore, E., 2012. The discovery of population differences in network community structure: new methods and applications to brain functional networks in schizophrenia. *NeuroImage* 59, 3889–3900.
- Aminoff, E.M., Kveraga, K., Bar, M., 2013. The role of the parahippocampal cortex in cognition. *Trends Cogn. Sci.* 17, 379–390.
- Amunts, K., Schleicher, A., Burgel, U., Mohlberg, H., Uylings, H.B., Zilles, K., 1999. Broca's region revisited: cytoarchitecture and intersubject variability. *J. Comp. Neurol.* 412, 319–341.
- Andrews-Hanna, J.R., Reidler, J.S., Sepulcre, J., Poulin, R., Buckner, R.L., 2010. Functional-anatomic fractionation of the brain's default network. *Neuron* 65, 550–562.
- Badre, D., Poldrack, R.A., Pare-Blagoev, E.J., Insler, R.Z., Wagner, A.D., 2005. Dissociable controlled retrieval and generalized selection mechanisms in ventrolateral prefrontal cortex. *Neuron* 47, 907–918.
- Barsalou, L.W., 1999. Perceptual symbol systems. *Behav. Brain Sci.* 22, 577–609 discussion 610–660.
- Barsalou, L.W., Kyle Simmons, W., Barbey, A.K., Wilson, C.D., 2003. Grounding conceptual knowledge in modality-specific systems. *Trends Cogn. Sci.* 7, 84–91.
- Berryhill, M.E., Phuong, L., Picasso, L., Cabeza, R., Olson, I.R., 2007. Parietal lobe and episodic memory: bilateral damage causes impaired free recall of autobiographical memory. *J. Neurosci.* 27, 14415–14423.
- Berwick, R.C., Friederici, A.D., Chomsky, N., Bolhuis, J.J., 2013. Evolution, brain, and the nature of language. *Trends Cogn. Sci.* 17, 89–98.
- Binder, J.R., Desai, R.H., 2011. The neurobiology of semantic memory. *Trends Cogn. Sci.* 15, 527–536.
- Binder, J.R., Frost, J.A., Hammeke, T.A., Bellgowan, P.S., Rao, S.M., Cox, R.W., 1999. Conceptual processing during the conscious resting state. A functional MRI study. *J. Cogn. Neurosci.* 11, 80–95.
- Binder, J.R., Westbury, C.F., McKiernan, K.A., Possing, E.T., Medler, D.A., 2005. Distinct brain systems for processing concrete and abstract concepts. *J. Cogn. Neurosci.* 17, 905–917.
- Binder, J.R., Desai, R.H., Graves, W.W., Conant, L.L., 2009. Where is the semantic system? A critical review and meta-analysis of 120 functional neuroimaging studies. *Cereb. Cortex* 19, 2767–2796.
- Biswal, B., Yetkin, F.Z., Haughton, V.M., Hyde, J.S., 1995. Functional connectivity in the motor cortex of resting human brain using echo-planar MRI. *Magn. Reson. Med.* 34, 537–541.
- Biswal, B.B., Mennes, M., Zuo, X.N., Gohel, S., Kelly, C., Smith, S.M., Beckmann, C.F., Adelstein, J.S., Buckner, R.L., Colcombe, S., Dogonowski, A.M., Ernst, M., Fair, D., Hampson, M., Hoptman, M.J., Hyde, J.S., Kiviniemi, V.J., Kotter, R., Li, S.J., Lin, C.P., Lowe, M.J., Mackay, C., Madden, D.J., Madsen, K.H., Margulies, D.S., Mayberg, H.S., McMahon, K., Monk, C.S., Mostofsky, S.H., Nagel, B.J., Pekar, J.J., Peltier, S.J., Petersen, S.E., Riedl, V., Rombouts, S.A., Rypma, B., Schlaggar, B.L., Schmidt, S., Seidler, R.D., Siegle, G.J., Sorg, C., Teng, G.J., Veijola, J., Villringer, A., Walter, M., Wang, L., Weng, X.C., Whitfield-Gabrieli, S., Williamson, P., Windischberger, C., Zang, Y.F., Zhang, H.Y., Castellanos, F.X., Milham, M.P., 2010. Toward discovery science of human brain function. *Proc. Natl. Acad. Sci. U. S. A.* 107, 4734–4739.
- Bonner, M.F., Peelle, J.E., Cook, P.A., Grossman, M., 2013. Heteromodal conceptual processing in the angular gyrus. *NeuroImage* 71, 175–186.
- Bontempi, B., Laurent-Demir, C., Destrade, C., Jaffard, R., 1999. Time-dependent reorganization of brain circuitry underlying long-term memory storage. *Nature* 400, 671–675.
- Boulenger, V., Hauk, O., Pulvermüller, F., 2009. Grasping ideas with the motor system: semantic somatotopy in idiom comprehension. *Cereb. Cortex* 19, 1905–1914.
- Bozeat, S., Lambon Ralph, M.A., Patterson, K., Garrard, P., Hodges, J.R., 2000. Non-verbal semantic impairment in semantic dementia. *Neuropsychologia* 38, 1207–1215.
- Braga, R.M., Sharp, D.J., Leeson, C., Wise, R.J., Leech, R., 2013. Echoes of the brain within default mode, association, and heteromodal cortices. *J. Neurosci.* 33, 14031–14039.
- Buckner, R.L., Carroll, D.C., 2007. Self-projection and the brain. *Trends Cogn. Sci.* 11, 49–57.
- Buckner, R.L., Andrews-Hanna, J.R., Schacter, D.L., 2008. The brain's default network: anatomy, function, and relevance to disease. *Ann. N. Y. Acad. Sci.* 1124, 1–38.

- Hart Jr, J., Gordon, B., 1990. Delineation of single-word semantic comprehension deficits in aphasia, with anatomical correlation. *Ann. Neurol.* 27, 226–231.
- Hassabis, D., Maguire, E.A., 2007. Deconstructing episodic memory with construction. *Trends Cogn. Sci.* 11, 299–306.
- He, Y., Wang, J., Wang, L., Chen, Z.J., Yan, C., Yang, H., Tang, H., Zhu, C., Gong, Q., Zang, Y., Evans, A.C., 2009. Uncovering intrinsic modular organization of spontaneous brain activity in humans. *PLoS One* 4, e5226.
- Hickok, G., Poeppel, D., 2007. The cortical organization of speech processing. *Nat. Rev. Neurosci.* 8, 393–402.
- Hodges, J.R., Patterson, K., Oxbury, S., Funnell, E., 1992. Semantic dementia. Progressive fluent aphasia with temporal lobe atrophy. *Brain* 115 (Pt 6), 1783–1806.
- Hoffman, P., 2015. The meaning of 'life' and other abstract words: Insights from neuropsychology. *J. Neuropsychol.*
- Humphreys, G.F., Lambon Ralph, M.A., 2014. Fusion and fission of cognitive functions in the human parietal cortex. *Cereb. Cortex.*
- Humphreys, G.F., Hoffman, P., Visser, M., Binney, R.J., Lambon Ralph, M.A., 2015. Establishing task- and modality-dependent dissociations between the semantic and default mode networks. *Proc. Natl. Acad. Sci. U. S. A.* 112, 7857–7862.
- Humphries, C., Binder, J.R., Medler, D.A., Liebenthal, E., 2007. Time course of semantic processes during sentence comprehension: an fMRI study. *NeuroImage* 36, 924–932.
- Jefferies, E., 2013. The neural basis of semantic cognition: converging evidence from neuropsychology, neuroimaging and TMS. *Cortex* 49, 611–625.
- Lambon Ralph, M.A., 2014. Neurocognitive insights on conceptual knowledge and its breakdown. *Philos. Trans. R. Soc. Lond. Ser. B Biol. Sci.* 369, 20120392.
- Lancaster, J.L., Tordesillas-Gutierrez, D., Martinez, M., Salinas, F., Evans, A., Zilles, K., Mazziotta, J.C., Fox, P.T., 2007. Bias between MNI and Talairach coordinates analyzed using the ICBM-152 brain template. *Hum. Brain Mapp.* 28, 1194–1205.
- Lauro, L.J., Tettamanti, M., Cappa, S.F., Papagno, C., 2008. Idiom comprehension: a prefrontal task? *Cereb. Cortex* 18, 162–170.
- Leech, R., Sharp, D.J., 2014. The role of the posterior cingulate cortex in cognition and disease. *Brain* 137, 12–32.
- Leech, R., Braga, R., Sharp, D.J., 2012. Echoes of the brain within the posterior cingulate cortex. *J. Neurosci.* 32, 215–222.
- Li, X., 1983. The distribution of left and right handedness in Chinese people. *Acta Psychol. Sin.* 3, 268–276.
- Lin, Q., Dai, Z., Xia, M., Han, Z., Huang, R., Gong, G., Liu, C., Bi, Y., He, Y., 2015. A connectivity-based test-retest dataset of multi-modal magnetic resonance imaging in young healthy adults. *Sci. Data* 2, 150056.
- Mantini, D., Gerits, A., Nelissen, K., Durand, J.B., Joly, O., Simone, L., Sawamura, H., Wardak, C., Orban, G.A., Buckner, R.L., Vanduffel, W., 2011. Default mode of brain function in monkeys. *J. Neurosci.* 31, 12954–12962.
- Maslov, S., Sneppen, K., 2002. Specificity and stability in topology of protein networks. *Science* 296, 910–913.
- Maviel, T., Durkin, T.P., Menzaghi, F., Bontempi, B., 2004. Sites of neocortical reorganization critical for remote spatial memory. *Science* 305, 96–99.
- McCandliss, B.D., Cohen, L., Dehaene, S., 2003. The visual word form area: expertise for reading in the fusiform gyrus. *Trends Cogn. Sci.* 7, 293–299.
- McClelland, J.L., McNaughton, B.L., O'Reilly, R.C., 1995. Why there are complementary learning-systems in the hippocampus and neocortex – insights from the successes and failures of connectionist models of learning and memory. *Psychol. Rev.* 102, 419–457.
- Murphy, K., Birn, R.M., Handwerker, D.A., Jones, T.B., Bandettini, P.A., 2009. The impact of global signal regression on resting state correlations: are anti-correlated networks introduced? *NeuroImage* 44, 893–905.
- Nadel, L., Moscovitch, M., 1997. Memory consolidation, retrograde amnesia and the hippocampal complex. *Curr. Opin. Neurobiol.* 7, 217–227.
- Newman, M.E., 2006a. Modularity and community structure in networks. *Proc. Natl. Acad. Sci. U. S. A.* 103, 8577–8582.
- Newman, M.E.J., 2006b. Finding community structure in networks using the eigenvectors of matrices. *Phys. Rev. E* 74.
- Newman, M.E.J., Girvan, M., 2004. Finding and evaluating community structure in networks. *Phys. Rev. E* 69.
- Noonan, K.A., Jefferies, E., Visser, M., Lambon Ralph, M.A., 2013. Going beyond inferior prefrontal involvement in semantic control: evidence for the additional contribution of dorsal angular gyrus and posterior middle temporal cortex. *J. Cogn. Neurosci.* 25, 1824–1850.
- Paivio, A., 1990. *Mental Representations*. Oxford University Press.
- Patterson, K., Nestor, P.J., Rogers, T.T., 2007. Where do you know what you know? The representation of semantic knowledge in the human brain. *Nat. Rev. Neurosci.* 8, 976–987.
- Pickering, M.J., Garrod, S., 2007. Do people use language production to make predictions during comprehension? *Trends Cogn. Sci.* 11, 105–110.
- Power, J.D., Cohen, A.L., Nelson, S.M., Wig, G.S., Barnes, K.A., Church, J.A., Vogel, A.C., Laumann, T.O., Miezin, F.M., Schlaggar, B.L., Petersen, S.E., 2011. Functional network organization of the human brain. *Neuron* 72, 665–678.
- Power, J.D., Barnes, K.A., Snyder, A.Z., Schlaggar, B.L., Petersen, S.E., 2012. Spurious but systematic correlations in functional connectivity MRI networks arise from subject motion. *NeuroImage* 59, 2142–2154.
- Power, J.D., Schlaggar, B.L., Lessov-Schlaggar, C.N., Petersen, S.E., 2013. Evidence for hubs in human functional brain networks. *Neuron* 79, 798–813.
- Price, A.R., Bonner, M.F., Peelle, J.E., Grossman, M., 2015. Converging evidence for the neuroanatomic basis of combinatorial semantics in the angular gyrus. *J. Neurosci.* 35, 3276–3284.
- Raichle, M.E., MacLeod, A.M., Snyder, A.Z., Powers, W.J., Gusnard, D.A., Shulman, G.L., 2001. A default mode of brain function. *Proc. Natl. Acad. Sci. U. S. A.* 98, 676–682.
- Ranganath, C., Ritchey, M., 2012. Two cortical systems for memory-guided behaviour. *Nat. Rev. Neurosci.* 13, 713–726.
- Renoult, L., Davidson, P.S., Palombo, D.J., Moscovitch, M., Levine, B., 2012. Personal semantics: at the crossroads of semantic and episodic memory. *Trends Cogn. Sci.* 16, 550–558.
- Rogers, T.T., Lambon Ralph, M.A., Garrard, P., Bozeat, S., McClelland, J.L., Hodges, J.R., Patterson, K., 2004. Structure and deterioration of semantic memory: a neuropsychological and computational investigation. *Psychol. Rev.* 111, 205–235.
- Rubinov, M., Sporns, O., 2010. Complex network measures of brain connectivity: uses and interpretations. *NeuroImage* 52, 1059–1069.
- Sabsevitz, D.S., Medler, D.A., Seidenberg, M., Binder, J.R., 2005. Modulation of the semantic system by word imageability. *NeuroImage* 27, 188–200.
- Saur, D., Kreher, B.W., Schnell, S., Kummerer, D., Kellmeyer, P., Vry, M.S., Umarova, R., Musso, M., Glauche, V., Abel, S., Huber, W., Rijntjes, M., Hennig, J., Weiller, C., 2008. Ventral and dorsal pathways for language. *Proc. Natl. Acad. Sci. U. S. A.* 105, 18035–18040.
- Schacter, D.L., Addis, D.R., Buckner, R.L., 2007. Remembering the past to imagine the future: the prospective brain. *Nat. Rev. Neurosci.* 8, 657–661.

- Wagner, A.D., Pare-Blagoev, E.J., Clark, J., Poldrack, R.A., 2001. Recovering meaning: left prefrontal cortex guides controlled semantic retrieval. *Neuron* 31, 329–338.
- Waites, A.B., Stanislavsky, A., Abbott, D.F., Jackson, G.D., 2005. Effect of prior cognitive state on resting state networks measured with functional connectivity. *Hum. Brain Mapp.* 24, 59–68.
- Wang, J., Conder, J.A., Blitzer, D.N., Shinkareva, S.V., 2010. Neural representation of abstract and concrete concepts: a meta-analysis of neuroimaging studies. *Hum. Brain Mapp.* 31, 1459–1468.
- Wang, Y., Nelissen, N., Adamczuk, K., De Weer, A.S., Vandenbulcke, M., Sunaert, S., Vandenberghe, R., Dupont, P., 2014. Reproducibility and robustness of graph measures of the associative-semantic network. *PLoS One* 9, e115215.
- Wang, J., Wang, X., Xia, M., Liao, X., Evans, A., He, Y., 2015. GRETNA: a graph theoretical network analysis toolbox for imaging connectomics. *Front. Hum. Neurosci.* 9, 386.
- Warrington, E.K., 1975. The selective impairment of semantic memory. *Q. J. Exp. Psychol.* 27, 635–657.
- Wei, T., Liang, X., He, Y., Zang, Y., Han, Z., Caramazza, A., Bi, Y., 2012. Predicting conceptual processing capacity from spontaneous neuronal activity of the left middle temporal gyrus. *J. Neurosci.* 32, 481–489.
- Whitney, C., Kirk, M., O'Sullivan, J., Lambon Ralph, M.A., Jefferies, E., 2011. The neural organization of semantic control: TMS evidence for a distributed network in left inferior frontal and posterior middle temporal gyrus. *Cereb. Cortex* 21, 1066–1075.
- Whitney, C., Kirk, M., O'Sullivan, J., Lambon Ralph, M.A., Jefferies, E., 2012. Executive semantic processing is underpinned by a large-scale neural network: revealing the contribution of left prefrontal, posterior temporal, and parietal cortex to controlled retrieval and selection using TMS. *J. Cogn. Neurosci.* 24, 133–147.
- Wig, G.S., Schlaggar, B.L., Petersen, S.E., 2011. Concepts and principles in the analysis of brain networks. *Ann. N. Y. Acad. Sci.* 1224, 126–146.
- Winocur, G., Moscovitch, M., Sekeres, M., 2007. Memory consolidation or transformation: context manipulation and hippocampal representations of memory. *Nat. Neurosci.* 10, 555–557.
- Wirth, M., Jann, K., Dierks, T., Federspiel, A., Wiest, R., Horn, H., 2011.